

Note on bimetric causal diagrams

Mikica Kocic

*Department of Physics & The Oskar Klein Centre,
Stockholm University, AlbaNova University Centre, SE-106 91 Stockholm*

E-mail: mikica.kocic@fysik.su.se

Abstract. A new kind of diagrams is presented, showing the causal structure of bimetric interactions.

Introduction. The metric configurations in de Rham–Gabadadze–Tolley massive gravity [1–3] and Hassan-Rosen bimetric theory [4, 5], can be classified in terms of the intersections of their null cones [6] (cf. [7]). The classification of causal types is shown in figure 1.

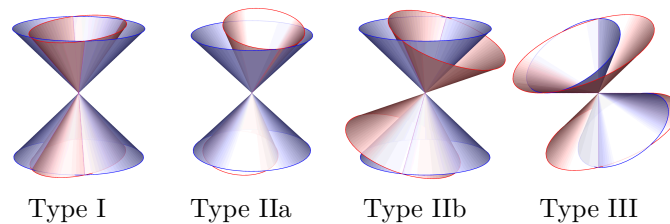


Figure 1. Null cones for possible metric configurations in the ghost-free bimetric theory and massive gravity [6]. Types IIa, IIb, and III are nonbidiagonalizable (the metrics cannot be simultaneously diagonalized). Type III is absent in spherical symmetry because of dimensional reduction.

An arbitrary coordinate transformation can only deform the null cones, keeping the nature of their intersections. Therefore, each point of bimetric spacetime carries a definite causal type which can be plotted in a diagram (as an indicator function), displaying an invariant picture of bimetric spacetime. An example is shown in figure 2, which illustrates a bimetric spherical dust collapse from [8]. The patches in the causal diagram highlight the relative dynamics of the metric fields showing their oscillations in space and time.

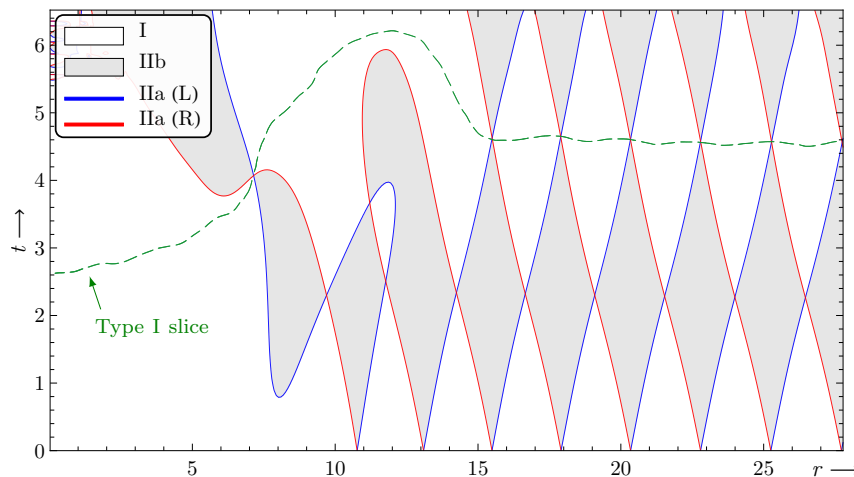


Figure 2. Causal diagram for a bimetric solution from [8]. The white regions are Type I, the shaded Type IIb, and the edges Type IIa. The dashed line is a bidiagonal (Type I) slice.

Construction. This section gives a procedure on how to plot a bimetric causal diagram in spherical symmetry, where every point in the diagram corresponds to a two-dimensional sphere. Consider two metrics of the following form,

$$g = -\alpha^2 dt^2 + A^2(dr + \beta dt)^2 + B^2 d\Omega^2,$$

$$f = -\tilde{\alpha}^2 dt^2 + \tilde{A}^2(dr + \tilde{\beta} dt)^2 + \tilde{B}^2 d\Omega^2.$$

Let r_L and r_R be the coordinates of the g null cone, and similarly \tilde{r}_L and \tilde{r}_R the coordinates of the f null cone, both cut at $\partial/\partial t$ in the tangent space (these coordinates can be obtained by setting $g, f, d\Omega = 0, dt = 1$, and then solving for dr),

$$r_L := -\beta - \alpha/A, \quad r_R := -\beta + \alpha/A, \quad r_L < r_R,$$

$$\tilde{r}_L := -\tilde{\beta} - \tilde{\alpha}/\tilde{A}, \quad \tilde{r}_R := -\tilde{\beta} + \tilde{\alpha}/\tilde{A}, \quad \tilde{r}_L < \tilde{r}_R.$$

Then, the causal type can be determined from the following two distances using table 1,

$$L_\Delta := r_L - \tilde{r}_L, \quad R_\Delta := r_R - \tilde{r}_R.$$

Table 1. Causal type discrimination based on L_Δ and R_Δ .

L_Δ	R_Δ	$L_\Delta R_\Delta$	Causal type	Comment
< 0	< 0	> 0	Type IIb	g left of f
< 0	$= 0$	$= 0$	Type IIa (R)	right null direction in common
< 0	> 0	< 0	Type I	f inside g
$= 0$	< 0	$= 0$	Type IIa (L)	left null direction in common
$= 0$	$= 0$	$= 0$	Type I	double null direction in common
$= 0$	> 0	$= 0$	Type IIa (L)	left null direction in common
> 0	< 0	< 0	Type I	g inside f
> 0	$= 0$	$= 0$	Type IIa (R)	right null direction in common
> 0	> 0	> 0	Type IIb	f left of g

The causal regions can be shown by plotting the product $L_\Delta R_\Delta$, in which case Type I regions have $L_\Delta R_\Delta < 0$, Type IIb regions $L_\Delta R_\Delta > 0$, and Type IIa regions have $L_\Delta R_\Delta = 0$ (Type I if it is a double zero). An example for the solution from figure 2 is shown in figure 3.

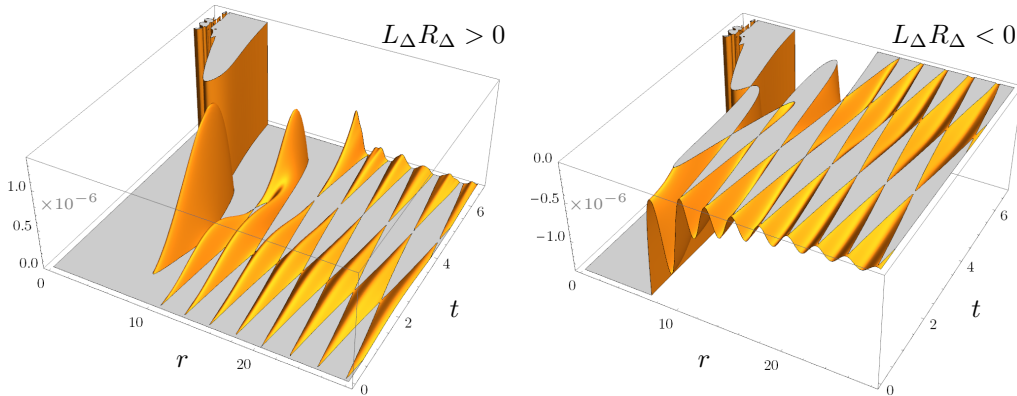


Figure 3. Discriminant $L_\Delta R_\Delta$ for the bimetric solution in figure 2.

Outlook. Note that L_Δ and R_Δ are smooth functions. Besides, the coordinate transformations can only smoothly deform the causal diagram: the imprinted topological features, such as which regions are adjacent to each other, can not be removed. Consequently, one can construct a “painted” Penrose–Carter diagram for each sector, depicting the relative causal structure between the two metrics. Finally, the causal types can be tracked along any curve (or surface) as shown in figure 4. For example, bidiagonal slices comprise Type I paths (not necessarily spacelike), illustrated by the dashed line in figure 2.

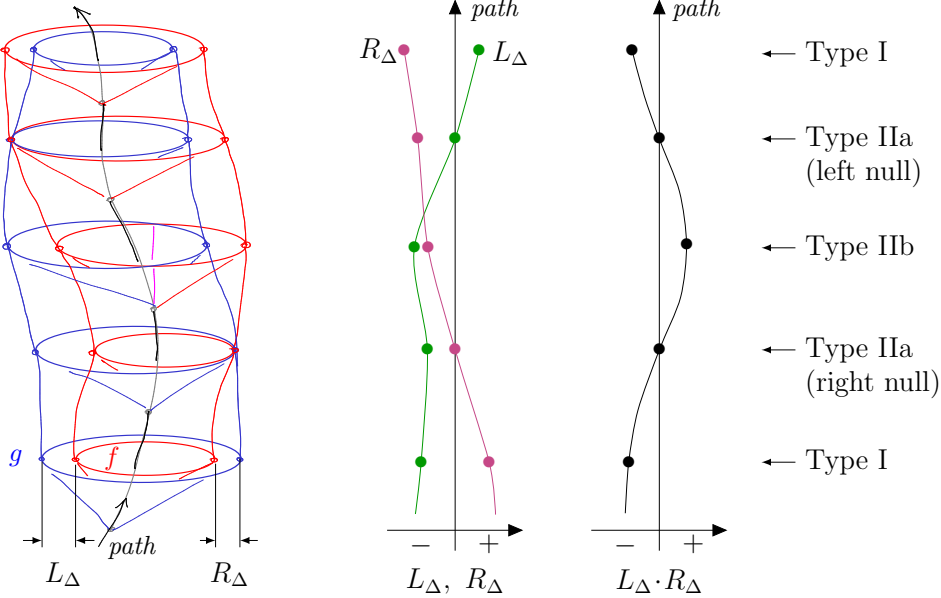


Figure 4. Tracking the causal type along an arbitrary path.

Acknowledgments. I wish to thank Fawad Hassan, Edvard Mörtzell, Francesco Torsello, Anders Lundkvist, and Marcus Högåås for the discussions and helpful comments.

References

- [1] C. de Rham and G. Gabadadze, *Generalization of the Fierz-Pauli Action*, *Phys. Rev.* **D82** (2010) 044020, [1007.0443].
- [2] C. de Rham, G. Gabadadze and A. J. Tolley, *Resummation of Massive Gravity*, *Phys. Rev. Lett.* **106** (2011) 231101, [1011.1232].
- [3] S. F. Hassan and R. A. Rosen, *Resolving the Ghost Problem in non-Linear Massive Gravity*, *Phys. Rev. Lett.* **108** (2012) 041101, [1106.3344].
- [4] S. F. Hassan and R. A. Rosen, *Bimetric Gravity from Ghost-free Massive Gravity*, *JHEP* **02** (2012) 126, [1109.3515].
- [5] S. F. Hassan and A. Lundkvist, *Analysis of constraints and their algebra in bimetric theory*, *JHEP* **08** (2018) 182, [1802.07267].
- [6] S. F. Hassan and M. Kocic, *On the local structure of spacetime in ghost-free bimetric theory and massive gravity*, *JHEP* **05** (2018) 099, [1706.07806].
- [7] D. Blas, C. Deffayet and J. Garriga, *Global structure of bigravity solutions*, *Class. Quant. Grav.* **23** (2006) 1697–1719, [hep-th/0508163].
- [8] M. Kocic, F. Torsello, M. Högåås and E. Mortsell, *Spherical dust collapse in bimetric relativity: Bimetric polytropes*, 1904.08617.